Investigation of the interaction between a β–cyclodextrin and DMPC liposomes: a small angle neutron scattering study.

Arnaud Joset [‡a], *Angeliki Grammenos*[‡b], *Maryse Hoebeke* [b], *Bernard Leyh* [a]

[a]Molecular Dynamics Laboratory, Department of Chemistry B6c, University of Liège,

Sart-Tilman, Belgium

[b]Biomedical Spectroscopy Laboratory, Department of Physics, B5a, University of Liège,

Sart-Tilman, Belgium

‡ Corresponding authors.

Email address: Arnaud.Joset@ulg.ac.be; *Tel.*: +32 (0)4 366 34 69; *Fax.*: +32 (0)4 366 34 97

The final publication is available at Springer via http://dx.doi.org/10.1007/s10847-015-0592-x

Abstract

The Small Angle Neutron Scattering technique (SANS) has been applied to investigate the interaction between a cyclodextrin (CD) and liposomes. From the modelling of the experimental neutron scattering cross sections, the detailed structure of dimyristoylphosphatidylcholine (DMPC) liposomes is assessed upon addition of increasing amounts of randomly methylated β-CD (RAMEB). This study has been performed at two temperatures bracketing the phase transition of the DMPC bilayers. The fraction of DMPC molecules incorporated into the vesicles is inferred. The dose-dependent phospholipidic extraction by RAMEB is quantified as well as the concomitant evolution of the liposome radius and of the thickness of the hydrophobic and hydrophilic parts of the membrane. The possible formation of CD-DMPC inclusion complexes is also assessed. The data suggest the dose-dependent coverage by RAMEB of the outer liposome interface. Our analysis highlights the important role of temperature on the mechanism of action of RAMEB. These results are discussed in the framework of the Area-Difference-Elasticity model.

KEYWORDS: cyclodextrins; dimyristoylphosphatidylcholine; vesicles; membranes; neutron scattering; structure

1 Introduction

Cyclodextrins (CD) were first described by Villiers in 1891[1,2]. However, Schardinger and Cramer, at the beginning of the 20th century, really laid the foundations of cyclodextrin chemistry [3,4]. They discovered three types of natural cyclodextrins (CD), α-, β- and γ-CD, which consist respectively of six, seven and eight glucopyranose units linked head-to-tail to build a ring and which adopt each the shape of a truncated cone. CD present an hydrophilic surface and a lipophilic central cavity leading to inclusion and non-inclusion complexes for a variety of host molecules [5,6]. Intensively investigated due to their cavitant properties, CD are nowadays widely used in the food, cosmetic, textile or pharmaceutical industry [7-14].

β-CD are prone to include cholesterol because their cavity size is sufficiently large [15]. As a consequence, they are relevant tools to investigate the plasma cell membrane and particularly the lipid raft function [16-18]. Several studies showed that cholesterol-containing membranes are more sensitive to methylated CD than to natural CD [16,19,20]. Among the former, the randomly methylated β-CD (RAMEB) passed all toxicological tests [16,19-23].

Despite several studies [24], the mechanism of action of RAMEB on cell membranes remains poorly understood. Most measurements focused only on the cholesterol extraction and did not address the possible competitive phospholipid removal which might also be of major importance. β-CD are widely used indeed in the presence of phospholipids and some recent investigations have pointed out that lipid desorption induced by CD can lead to the formation of aggregates with solubilizing properties[25,26]. The understanding of CD action on phospholipid membranes is thus of the highest importance. In this paper, we investigate the interaction between a methylated β-CD and a model membrane using the Small-Angle Neutron Scattering technique (SANS), which is a powerful method to investigate model membranes [27-36]. This technique will first be applied to analyze the interaction between RAMEB and liposomes containing only phospholipids. In a second paper, the interaction between cyclodextrins (RAMEB) and cholesterol-doped liposomes will be addressed.

In a previous work, our group focused on the evaluation of the RAMEB action directly on cell membranes using electron spin resonance [37]. A more common way to evaluate the damage

caused by a CD on biomembranes is to use a lipid assay kit [16]. As the CD action on natural membranes is extremely complex, the use of models consisting of lipid bilayers is a relevant approach to reach a better understanding of the involved processes. Liposomes represent such an appropriate model. In addition to mimicking the membrane, liposomes can also be used as drug enhancers [38-43]. Another field also uses cyclodextrins as drug release modulators within liposomes [44-46].

Various techniques have been applied in order to understand the influence of CD on the stability as well as on the integrity of vesicle bilayers. Electron spin resonance highlighted the microviscosity changes induced by CD on liposome membranes [37]. The release of a fluorescent probe initially encapsulated in the liposomes has been used to evaluate the liposome integrity in contact with different amounts of CD [47]. Turbidity measurements have been performed to quantify the lipid leakage induced by CD on the liposome bilayer [19]. The structural changes were also assessed using differential scanning calorimetry [48], freeze-fracture electron microscopy [47], binding isotherms [49] or photon-correlation spectroscopy [19,23,49,50]. Despite all these studies, rare are those involving specifically the interaction between β-CD and phospholipids [19,49,51]. And, to the best of our knowledge, only information on the global liposome size and dispersity could be inferred from the previously mentioned techniques which do not give access to the internal structure of the bilayer.

The SANS technique is a powerful way to infer, from the modelling of the experimental neutron scattering cross sections, the detailed liposome structure which we define by the following parameters: average radius, thickness of both the hydrophobic and hydrophilic parts of the liposome bilayer, and liposome size polydispersity. In the present work, the evolution of these parameters has been monitored as a function of RAMEB concentration. The possible coverage by the RAMEB molecules at the liposome-water interface was also considered.

Because of the existence of a phase transition associated with a change in the conformational order of the phospholipid acyl chains influencing the membrane fluidity [52], the influence of RAMEB on the liposome structure was considered at two temperatures (above and below the bilayer phase transition). In this study, we selected liposomes resulting from the self-assembling

of dimyristoylphosphatidylcholine (DMPC) which have a phase transition temperature close to 23°C. Dynamic light scattering (DLS) and surface tension measurements were performed in parallel to the SANS investigation.

2 Materials and methods

2.1 Liposome preparation

Dimyristoylphosphatidylcholine (DMPC) and octadecylamine (also called stearylamine , SA) were purchased from Sigma (Aldrich, Belgium) and were used without further purification. Phospholipid vesicles were prepared by hydration of lipid films as described by Hope et al. [53]. DMPC was first dissolved in chloroform to a concentration of 7.4 mM. The liposomes contained a molar fraction of 90% of DMPC (4.5 mg/mL) and were doped with 10% of SA (0.2 mg/mL): SA was added to the vesicles in order to prevent their spontaneous fusion, which is known to appear above the DMPC bilayer phase transition temperature [54]. The chloroform/phospholipid mixture was then stirred for 5 min and the solvent was evaporated under vacuum. The resulting lipid film was suspended in deuterium oxide (Sigma Aldrich, Belgium), and stirred by a vortex mixer in order to obtain large multilamellar vesicles (MLV) [55]. After hydration, five freeze-thaw cycles using liquid nitrogen were carried out to allow a better incorporation of the SA into the liposome phospholipidic bilayers. The MLV suspension was then transferred into an extruder (Lipex Biomembrane, Canada) with two (stacked) polycarbonate filters (0.1 μm pore size, Nucleopore, CA), under a pressure gradient up to 6800Pa of nitrogen (Air Liquide, Belgium). The procedure was repeated ten times at 35°C and resulted in unilamellar liposomes, as demonstrated by Olson et al. [56]. Once prepared, the liposomes were incubated with RAMEB (degree of substitution equal to 12.6; purchased fromWacker Chemie GmbH, Germany) at selected concentrations. The RAMEB solution had been first filtered on a microfilter with a pore size of 0.2 μm.

2.2 Surface Tension Measurements

Aqueous RAMEB solutions were prepared at various concentrations in the 10^{-5} to 10^{-1} M range. Surface tension measurements were collected in multi-well plates supplied with a MicroTrough S (Kibron, Germany) apparatus. Each plate contained 15 wells with a volume of 500 µl each and the data collection was performed with the Film Ware software (version 3.4). Each measurement was repeated 15 times at room temperature.

2.3 Dynamic Light Scattering (DLS)

DLS measurements were carried out with a particle size analyzer (Delsa Nano C, Particle Analyzer, Beckman Coulter) at a fixed scattering angle of 165°. The light source is a diode laser operating at λ=658 nm and 30 mW power. Measurements on the DMPC-liposome solutions in contact with different amounts of RAMEB were performed at two different temperatures (14 and 34°C) in duplicate. Each measure lasted about 20 minutes. Initially the liposome and RAMEB solutions were both filtered on a microfilter with a pore size of 0.2 µm. Data were handled using the CONTIN algorithm using the Delsa Nano software. At least four individual histograms were averaged leading to smooth distributions.

2.4 Small-Angle Neutron Scattering (SANS)

The SANS cross-sections of unilamellar DMPC vesicles in D_2O in contact with different concentrations of RAMEB were collected at the Jülich Centre for Neutron Science (JCNS) at two temperatures: 14°C and 34°C. The KWS1 and KWS2 small-angle instruments were used to collect data at three sample-detector distances: 2, 8 and 20m. The neutron wavelength, λ, was equal to 6.00 Å ± 0.60 Å after mechanical velocity selection. These conditions correspond to a momentum transfer range, q, from 2.36 10^{-3} Å^{-1} to 1.96 10^{-1} Å^{-1} where $q = {}^{4\pi}/_{\lambda} \sin(\theta)$ and 2θ is the scattering angle.

The scattered neutrons were detected on a two-dimensional ^{6}Li scintillation counter. Radial averaging led to a one-dimensional scattering function *I(q)*. The incoherent background was removed using a blank sample. Corrections for the background and sample holder contributions

were carried out according to standard data handling procedures (see, e.g. [57]. The data corresponding to the liposome solutions and to the pure solvent (D_2O) were handled in an identical way, and the scattering intensities were converted to macroscopic scattering cross-sections per unit volume, $d\Sigma/d\Omega$ (cm^{-1}), using calibration with a Poly(methyl methacrylate) sample. The liposome contribution was obtained by subtracting the cross section of the solvent, weighted by its volume fraction.

2.5 SANS Data handling

The liposomes are assumed to be spherical, consisting of concentric shells of mean radius *R*. The inner hydrophilic shell, the hydrophobic shell and the outer hydrophilic shell thicknesses are respectively denoted as d_{in}, *D,* and d_{out}. (Fig. 1a) The macroscopic scattering cross-section for the liposomes is given by the following formula

$$\frac{d\Sigma}{d\Omega} = \frac{[DMPC]\, N_A 10^{-3}}{\langle N \rangle} \int_0^\infty |A(q)|^2 P_n(R) dR \quad (1)$$

with $\langle N \rangle = \int_0^\infty N(R) P_n(R) dR$

where [*DMPC*] is the total DMPC concentration in *mol/L*, *N*(*R*) is the aggregation number of liposomes with radius *R* and $P_n(R)$ represents the liposome size distribution. Because the liposome solution was sufficiently diluted, the interferences between waves scattered by different liposomes may be ignored [58]. The scattering amplitude *A(q)* is given by

$$A(q) = 4\pi \int_{liposome} \tilde{\rho}\ (r) \frac{\sin(qr)}{qr} r^2\, dr \quad (2)$$

where the excess scattering length density $\tilde{\rho}$ is a function of the distance *r* from the center of the liposome and is equal to

$$\tilde{\rho}(r) = \tilde{\rho}_{SA}\varphi_{SA}(r) + \tilde{\rho}_{DMPC}\varphi_{DMPC}(r) \qquad (3)$$

We define as elementary scatterers the respective hydrophobic tails and hydrophilic heads of SA and DMPC. Depending on the zone of the liposome considered, $\tilde{\rho}_{SA}$and $\tilde{\rho}_{DMPC}$correspond to the excess scattering length density of the head or tail of the molecules. φ_{SA} and φ_{DMPC} are their respective volume fractions. A linear water penetration profile is assumed in the polar parts of the DMPC/SA bilayer (Fig. 1b). When cyclodextrin was added, its possible presence at the liposome/water interface has been included in the model in the following way. An additional layer with a thickness equal to 7.8Å [59], that is the height of a β–CD molecule, is considered. The scattering length density for this layer is calculated assuming a variable volume fraction of cyclodextrin within this layer which is otherwise filled by the water solvent. This volume fraction is then an additional fitting parameter.

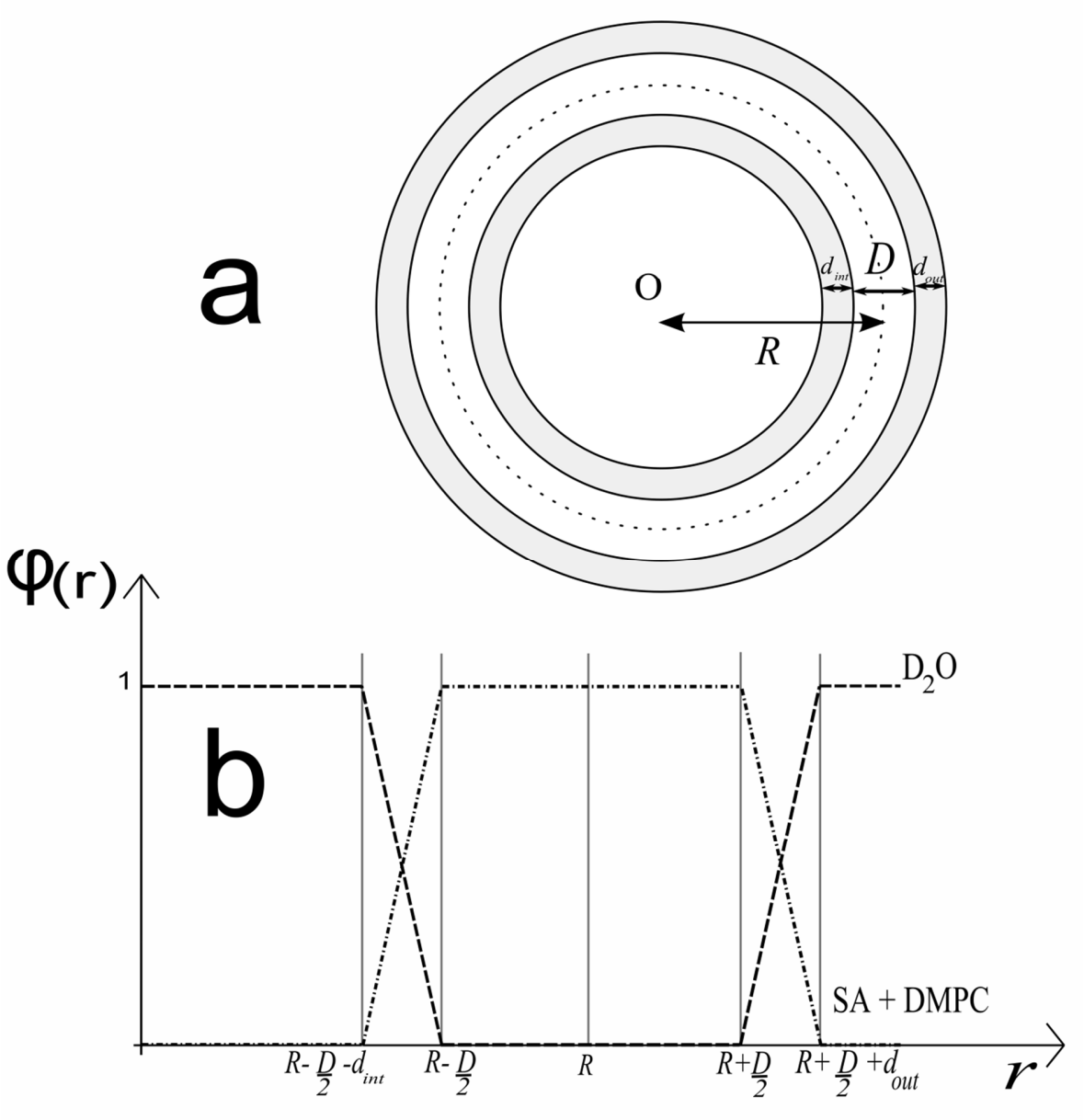

Fig. 1(a) Structure of a modelled liposome (see text for details); (b) Volume fraction of the DMPC/SA constituents of the liposome as a function of the distance from the center of the liposome (dash-dotted line). The volume fraction of water is shown as a dashed line. The CD fraction is not shown.

The following size distribution, inspired from the analysis of the vesicle size obtained by Hope et al. (1985) [53], has been used

$$P_n(z) = C\ \exp(-e^{-z} - z + 1) \quad (3)$$

$$z = \frac{R - R_c}{\sigma} \quad (4)$$

where C is a normalization coefficient. The average radius is then given by $\langle R \rangle = R_c + 0.577\sigma$ and the standard deviation, δ, is proportional to σ: $\delta = 1.283\sigma$.

As will be discussed later, the addition of RAMEB leads to the partial disruption of the liposomes and to the possible formation of inclusion complexes between RAMEB molecules and extracted DMPC chains. The contribution of these complexes to the scattering cross section has to be also considered. Based on the work of Anderson et al. [60] who detected 4:1 RAMEB - 1-palmitoyl-2-oleoyl-sn-glycero-3-phosphocholine (POPC) CD-POPC complexes, we assumed that 4:1 RAMEB-DMPC might be present and we modelled them as homogeneous spheres with a volume equal to four times the volume of a RAMEB molecule and with a scattering length density estimated from the atomic composition of the RAMEB and DMPC molecules. As the contribution of these complexes is not expected to be large, it does not seem relevant to implement a most sophisticated model. This contribution is then simply weighted by an additional fitting parameter and added to the liposome cross section.

The model depends therefore on five independent parameters, that is: (i) the average radius of the liposome ($\langle R \rangle$), (ii) the standard deviation of the radius, (iii) the thickness of the hydrophobic part (D), (iv) the volume fraction of RAMEB covering the surface of the vesicles (φ), and (v) the weighting factor of the contribution of the RAMEB-DMPC inclusion complexes. The other parameters are not independent. The knowledge of R and D leads to the volume of the hydrophobic shell, from which the aggregation number (number of individual amphiphilic molecules that are self-assembled in the vesicle) can be calculated based on the individual molecular volumes of the hydrophobic scatterers. The knowledge of the aggregation number, of the scatterer volumes, and of the volume fractions (see Fig. 1b) makes the calculation of d_{out} and d_{in}, possible.

Equation (1) involves the DMPC total concentration. However, due to the extrusion steps, the final total DMPC concentration is not precisely known. Part of the material must be retained by the polycarbonate filter during the repeated extrusion steps (see Material and methods). The actual final concentration of DMPC chains incorporated into the liposomes is related to the initial one (7.4 mM) via a correcting multiplying factor, denoted as m ($m \leq 1$). This factor, which results from the data fits, may also account for the possibility of (i) unassociated free DMPC chains which are too small to be seen in SANS and (ii) other types of self-assembled objects, like clusters of liposomes, whose size would be too large for them to be detected in our limited q range.

The total scattering cross section is then convoluted with an apparatus function in order to take into account the experimental resolution (see experimental part). A triangular shape has been assumed for the scattering vector spread ($\Delta q/q$ = 10%). The resulting model cross sections are then fitted to the experimental scattering curves and the quality of the fit has been monitored by calculating the χ^2 both in linear and in logarithmic mode.

2.6 Comparison of SANS and DLS size distributions

The analysis of the SANS data provides us with a number-weighted radius distribution, denoted P_n. The CONTIN algorithm used for the DLS data analysis leads to an intensity-weighted distribution, P_i, of the hydrodynamic radius. These two distributions are not equivalent but may be connected through the following equation [61,62]:

$$P_n = \frac{P_i}{[M(R)]^2 F(q;R)} \qquad (5)$$

where $M(R)$ is the molecular weight of a vesicle of radius R. $M(R)$ is proportional to the square of the vesicle radius:

$$M(R) = 4\pi R^2 \widetilde{D} \bar{\rho} \qquad (6)$$

where $\widetilde{D}$ represents the global thickness and $\bar{\rho}$ the average density of the bilayer. $F(q;R)$ is the form factor of the vesicle at the q value corresponding to the wavelength and detection angle of

the DLS instrument. Because all the information required to calculate $F(q;R)$ is available from the analysis of our SANS data, we found more consistent and practical to convert the P_n SANS distributions to P_i distributions which are comparable to the DLS distributions. This makes an easy and relevant comparison between DLS and SANS data possible, as will be discussed in Section 3. It must be emphasized that the liposome radii obtained by averaging over P_i are as a rule larger than those obtained from P_n because of the R^2 weighting factor appearing in equation (6). This has to be kept in mind when comparing different figures of the discussion section.

3 *Results and discussion*

Typical SANS cross-sections of DMPC vesicles without and with added RAMEB (at a concentration of 20 mM) as well as fits using the model described in Section 2.5 are displayed in Fig. 2. A good agreement is observed between the experimental and fitted data.

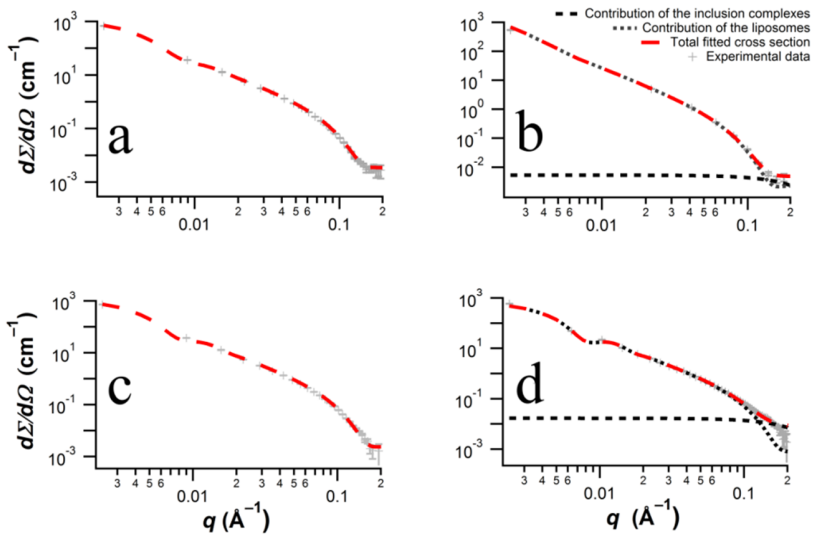

Fig. 2 Experimental macroscopic cross-sections of the liposomes (+ gray symbols) and their fits to the analytical model described in section 2.5 (red dotted line). The individual contribution of RAMEB-DMPC inclusion complexes is displayed as a black dotted line. (a) Pure liposomes at 14°C; (b) Liposomes at 14°C in contact with RAMEB at a concentration of 20 mM; (c) Pure liposomes at 34°C; (d) Liposomes in contact with RAMEB at a concentration of 20 mM at 34°C.

3.1 Fraction of DMPC molecules included in the unilamellar liposomes

The m parameter defined in Section 2.5 represents the fraction of the DMPC molecules which are actually included in liposomes. Three phenomena may be responsible for m values lower than unity: (i) the loss of DMPC material during the extrusion procedure, (ii) the presence of unassociated DMPC chains, and (iii) aggregation processes leading to structures which are too large to be detected in our q range. As RAMEB was added at the last step of the sample preparation procedure, the contribution of process (i) is the same for all samples. Relevant information may therefore be inferred about the possible additional influence of RAMEB on processes (ii) and (iii) globally, from the evolution of the m/m_0 parameter upon increasing RAMEB concentration at 14°C and 34°C (Fig. 3). m_0 is the value of m in the absence of RAMEB.

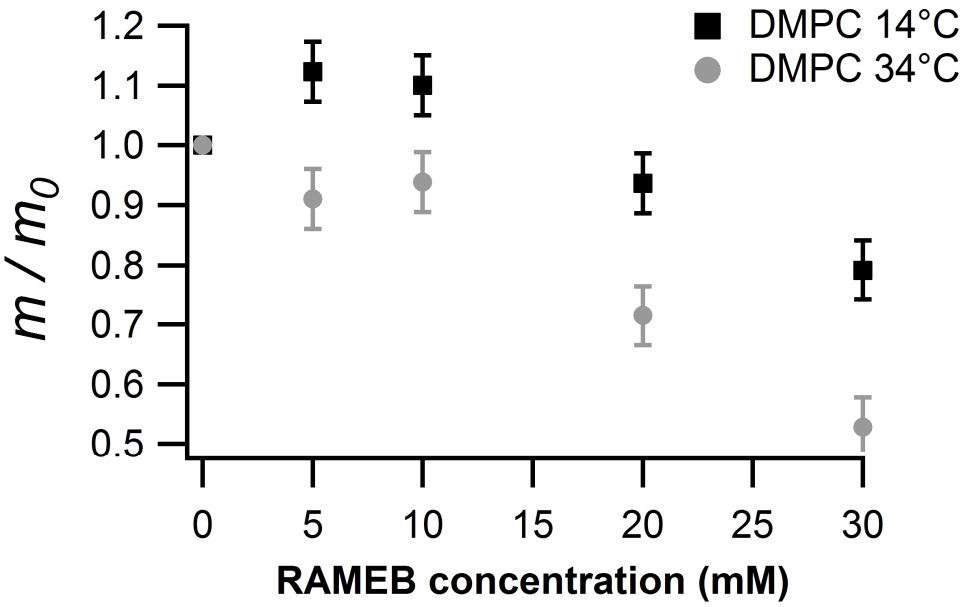

Fig. 3 Influence of RAMEB on the fraction of DMPC molecules included in the liposomes (m/m_0 parameter) at 14°C (black squares) and 34°C (grey dots)

Up to 10 mM of RAMEB, no significant variation of m/m_0 is detected within experimental limits. The slight increase from 1.0 to 1.12±0.05 in the [RAMEB] = 0 – 10 mM range at 14°C lies at the limit of experimental significance. It may be either assigned to experimental uncertainties or to a possible de-clustering of initially undetectable aggregated liposomes, leading to an increase of the cross section in the sampled q range. The most significant effect is, however, a regular linear decrease which takes place above 10 mM of CD for both temperatures. 21 ± 5 % of the initial liposomes are no longer detected at [RAMEB] = 30 mM at 14°C. At 34°C, this amount becomes even larger, 47 ± 5%. This effect is assigned to the solubilization of part of the liposomes resulting from the extraction of DMPC phospholipid chains by the β-CD, in agreement with the conclusions drawn by Hatzi and coworkers [19]. This extraction is made in a dose-dependent way and may lead either to aggregates composed of RAMEB and phospholipids that become larger with increasing RAMEB concentration [21,37] or to solubilized chains encapsulated by cyclodextrins [60] which provide a small contribution to the scattering cross section. As explained in section 2.5, we modelled this contribution by assuming, following

Anderson et al [60] a 4:1 stoechiometry for the RAMEB-DMPC complexes and by describing them as homogeneous spheres [63]. This contribution is displayed as black dotted lines in Fig. 2. It must be emphasized at this point that isolated DMPC or RAMEB molecules cannot be detected: they would lead to a scattering cross section in the 10^{-4} cm^{-1} range at q = 0, which corresponds to the noise level. Based on the cross section at q = 0 for this contribution and on the relevant scattering length values, the concentration of the inclusion complexes and therefore, the fraction of DMPC molecules included into these complexes can be inferred. The accuracy of these data is, however, limited, due to the small associated cross section. At [RAMEB] = 30 mM, the inclusion complex concentration is estimated to be 2.3±1.7 mM and 3.8±1.3mM at 14°C and 34°C, respectively. Compared to the total concentration of 7.4 mM, this corresponds to 31% and 51%. These values compare favorably with the above-cited values of 21% and 47% inferred above from the m/m_0 parameter, taking into account (i) the low accuracy of the determined inclusion complex cross section, and (ii) the fact that part of the DMPC molecules are lost during the extrusion process. Despite these caveats, these data suggest that DMPC extraction by RAMEB leading to inclusion complexes is probably one important mechanism operating under our experimental conditions.

Surface tension measurements were also performed, showing that RAMEB is able to weakly cluster above 15 ± 2 mM in agreement with Messner et al. [26]. These observations and the fact that no significant liposome solubilization is observed below 10 mM of RAMEB suggest that CD-clusters might also play a role in the liposome destruction.

The more efficient solubilization observed above the transition temperature is linked to the larger mobility of the DMPC chains in the fluid phase.

3.2 Liposome Radius, aggregation Number, and polydispersity

The evolution of the average radius of the surviving liposomes inferred from SANS upon addition of increasing amounts of RAMEB is shown in Fig. 4a. Without RAMEB addition, the average radius and aggregation number are identical below and above the transition temperature. This situation results directly from the extrusion procedure which governs the size distribution. These results are also in agreement with Kiselev et al. [64]. As soon as RAMEB is added,

temperature is seen to influence the liposome size evolution: below the DMPC transition temperature, the average liposome radius increases upon addition of CD whereas it remains nearly constant at 34°C.

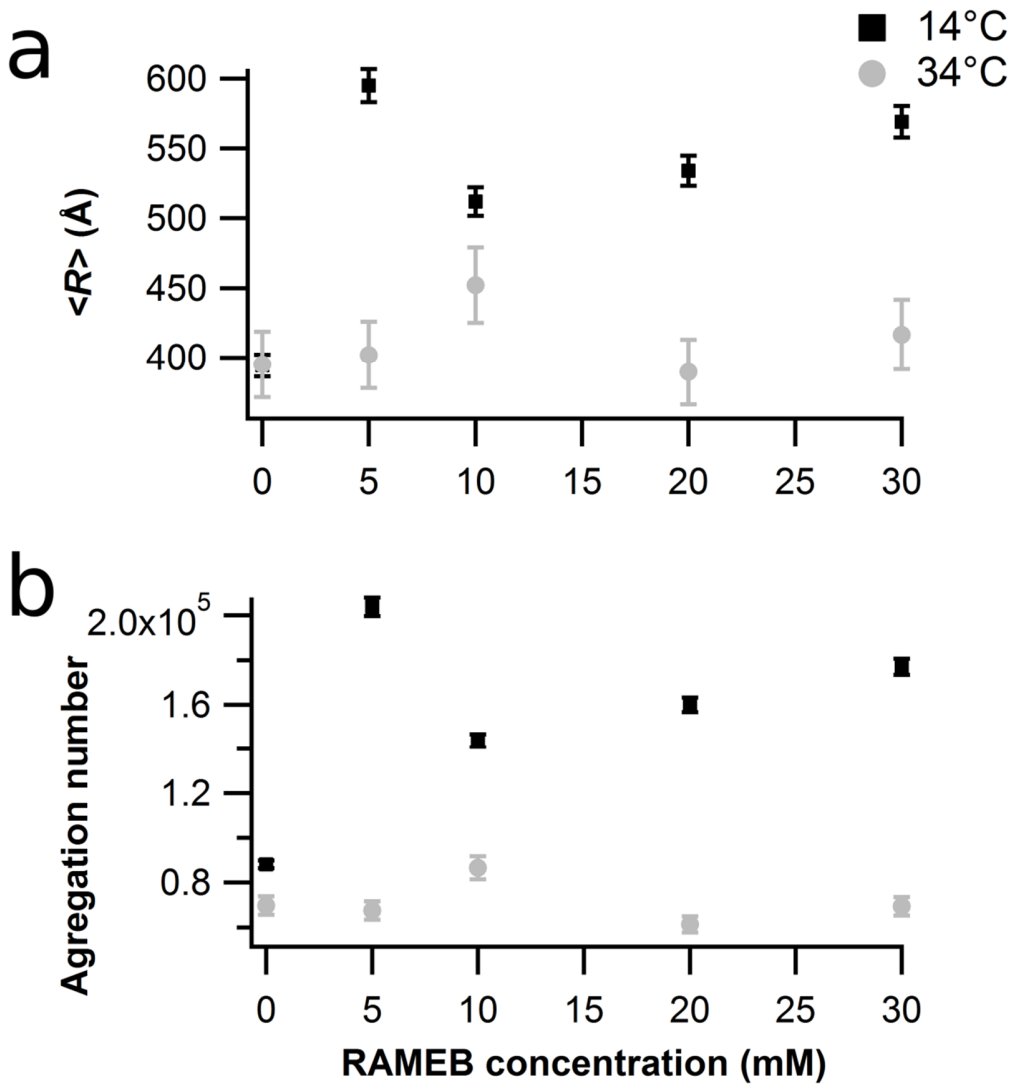

Fig. 4 Average liposome radius (a) and aggregation number (b) at different RAMEB concentrations at 14°C (black squares) and 34°C (grey dots). Note that the displayed radii are obtained by averaging over a number-weighted size distribution.

The evolution of the average size of the surviving liposomes is logically linked to that of the average aggregation number as shown in Fig. 4b.

Fig. 5a displays the influence of RAMEB on the liposome polydispersity. An increase is highlighted at 14°C but at 34°C the polydispersity is not significantly affected. This evolution is directly visible on the SANS cross sections displayed in Fig. 2.

This behavior as a function of the RAMEB concentration and of temperature is confirmed by DLS measurements (Fig. 5b and 5c). We recall here that the SANS size distributions have been converted into intensity-weighted distributions to make them comparable with the distributions inferred from DLS. As alluded to in Section 2.6, this is the reason why the maxima of the distributions in Figs. 5b and 5c correspond to larger radii than the average values of Fig. 4a, e.g. 395 Å (Fig. 4a) compared to 490 Å (Fig. 5b).

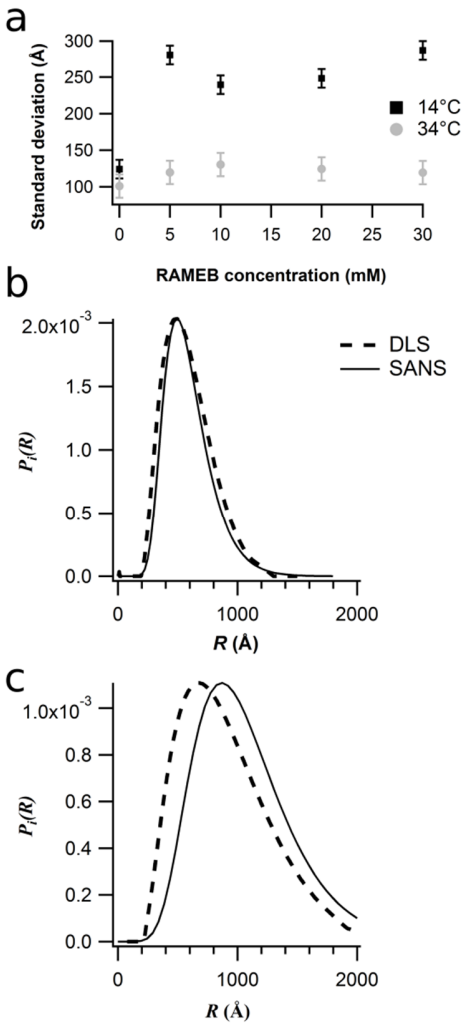

Fig. 5 (a) Standard deviation of the radius of the DMPC liposomes at 14°C (black squares) and 34°C (grey dots), as inferred from SANS, as a function of RAMEB concentration. (b) Liposome radius distribution at 14°C determined by DLS (dotted line) and SANS (solid line) for pure liposomes and (c) for liposomes in contact with RAMEB at a concentration of 20 mM. The SANS size distributions have been converted into intensity-weighted distributions, $P_i(R)$, to make them comparable with the distributions inferred from DLS

3.2.1 Below the DMPC transition temperature

Because it is well accepted that CD are not able to penetrate into phospholipid membranes [6,13,65], the increase in liposome size at 14°C could not be explained by a CD inclusion into the bilayer. We suggest that DMPC extraction by RAMEB leads to preferential destruction of the

small vesicles so that the size distribution of the surviving liposomes is shifted towards larger R values. As will be discussed below (Section 3.2.3), small liposomes have a larger curvature and a higher elastic energy, so that phospholipid extraction by CD favors their solubilization compared to larger ones.

However, because an increase of the polydispersity is also observed, this mechanism cannot be the only one which operates. It might be suggested that the DMPC molecules from small disrupted liposomes partly become included into the RAMEB-DMPC inclusion complexes discussed above and partly contribute to the formation of larger, more stable liposomes which would be responsible for the increased polydispersity. It has been proposed by Puskas and Csempesz that cyclodextrins may induce aggregation/or fusion of the vesicles [66]. This hypothesis is also compatible with the shift in the size distribution towards larger R values as observed on Fig. 4a.

The comparison of Figs. 3 and 4a shows that the conclusions drawn from both the m/m_0 and R parameters are compatible. A RAMEB concentration of 7.5 ± 2.5 mM must be reached in order that a significant effect is observed.

3.2.2 Above the DMPC transition temperature

Figs. 3 and 4 lead us to the conclusion that, at 34°C, (i) the fraction of DMPC molecules within unilamellar liposomes decreases upon RAMEB addition but that (ii) the average vesicle size is not significantly affected by the interactions with the CD.

These observations lead us to the hypothesis that phospholipid extraction above the DMPC bilayer transition temperature disrupts the liposomes to about the same extent whatever their size, contrarily to the situation prevailing below the transition temperature. As a consequence, the size distribution remains more or less unaffected and the average radius change is negligible.

3.2.3 Comparison between the behaviors below and above the transition temperature

A double question arises. Why do small liposomes become more easily disrupted than bigger ones below the gel-fluid transition temperature? Why does this differentiated behavior vanish above the transition temperature?

Bending a bilayer has an energy cost. In the frame of the Area-Difference-Elasticity (ADE) model [67], the total elastic energy, E_B, of a bilayer of fixed mean area A is written as

$$E_B = \frac{1}{2}\kappa \int_A dA'(C_1 + C_2)^2 + \frac{\alpha\pi\kappa}{2D^2 A}(\Delta A - \Delta A_0)^2 \qquad (7)$$

where κ is the bending modulus, C_1 and C_2 are the local curvatures along the two principal directions, D is the bilayer thickness, α is a constant which depends on the phospholipid and which is close to unity. ΔA_0 is the area difference between the outer and inner unstressed monolayers, due to the different numbers of phospholipid molecules they may contain, whereas ΔA is the actual area difference within the liposome. The first term of equation (7) is the Helfrich bending energy [68], at fixed bilayer area, whereas the second contribution takes into account the fact that bending a bilayer involves stretching the outer monolayer and compressing the inner one.

Equation (7) is strictly valid a 0 K. At finite temperatures, it becomes necessary to consider the membrane fluctuations through the renormalized bending energy [69,70]. The size distribution of a system of vesicles has been shown to depend exponentially on the renormalized bending energy, $E_B(R)$ divided by the thermal energy k_BT [69]. This renormalized bending energy takes into account the fact that membrane undulations at finite temperature lower the free energy uptake associated with the membrane bending required to build a vesicle. Vesicles of radius R close to the undulation wavelength will be formed preferentially. The effective, renormalized bending modulus decreases with the characteristic length scale of the vesicle, so that for

$$R \approx \widetilde{D}\ exp\left(\frac{4\pi}{3}\frac{\kappa}{k_BT}\right) \qquad (8)$$

where κ is the not renormalized bending modulus, the renormalized bending modulus is close to zero [70]. κ has been observed to decrease by about two orders of magnitude at the transition temperature [70].

Equations (7) and (8) provide two possible, and not mutually exclusive, explanations for the observed temperature-dependent behavior. First, our liposome preparation procedure leads to unilamellar spherical liposomes with an average radius of 400 Å and a moderately narrow size distribution (Fig. 5). Despite their bending, they are kinetically stabilized, in particular through the insertion of stearylammonium chains. Below the transition temperature, due to the large κ value, the bending energy is expected to vary significantly through the sampled *R* range, so that the smaller vesicles are much less stable and more prone to disruption following RAMEB-induced phospholipid extraction. Bilayer reorganization and formation of larger vesicles are expected to take place as inferred from the increase of the liposome polydispersity. Above the transition temperature, the Helfrich energy is much smaller due to the above-mentioned decrease of the bending modulus, so that the stability differences for different radii are significantly attenuated. The extraction of DMPC chains by RAMEB is probably favored by the higher mobility of the phospholipid chains (as we already pointed out when analyzing the m/m_0 parameter) but all vesicle sizes tend to be affected in a similar way.

A second contribution may arise from the second term of equation (7). Extraction of DMPC molecules by RAMEB involves necessarily the outer monolayer so that ΔA_0 decreases leading to an increase of $\frac{\kappa}{A}(\Delta A - \Delta A_0)^2$. This effect will be particularly important for small liposomes (small mean area *A*) and in the gel phase (large κ). This is also compatible with the observed behavior.

3.2.4 Coverage of the liposome external layer by RAMEB

Another parameter derived from the data modelling is the volume fraction of RAMEB covering the liposome surface. Fig. 6 highlights the dose dependent covering of liposomes by RAMEB. The coverage levels off at a volume fraction of about 0.5 and the largest increase takes

place between [RAMEB] = 0 and 10 mM. This can be correlated to the threshold observed in Fig. 3 for efficient DMPC extraction. When 30 mM of RAMEB is reached, half of the vesicle surface is covered. An adsorption of native-CD on membranes has been previously reported [71] and explained by an hydrogen bond formation between the phospholipidic polar head group and one hydroxyl group of the CD. RAMEB, however, possesses less –OH groups, which are replaced by methyl groups, so that the interaction with DMPC is expected to be weaker. As a matter of fact, our data do not provide us with any information on the strength of the link between the RAMEB molecules and the liposome outer surface. The fact that a large molar excess of RAMEB with respect to DMPC is used and that evidence for inclusion complexes has been found, which pleads for reasonable interaction energies, may justify a relatively large volume fraction of RAMEB at the liposome-water interface.

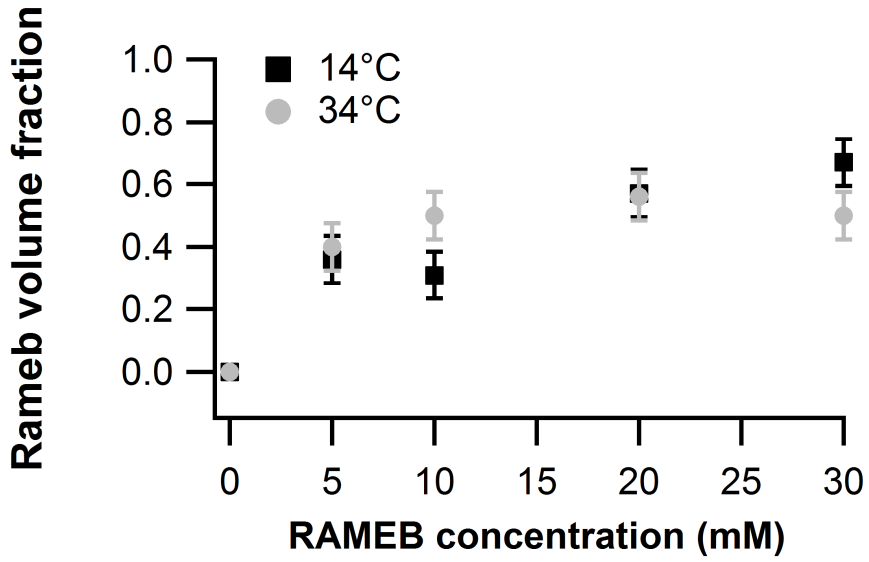

Fig. 6 Volume fraction of RAMEB on the liposome surface at 14°C (black squares) and 34°C (grey dots)

3.3 Bilayer thickness

The detailed liposome bilayer structure has also been assessed. Fig. 7 shows how the hydrophilic (Fig. 7a) and hydrophobic (Fig. 7b) sublayers of the membrane vary as a function of

the RAMEB concentration. Note that *d* is the average thickness of the inner and outer hydrophilic sublayers.

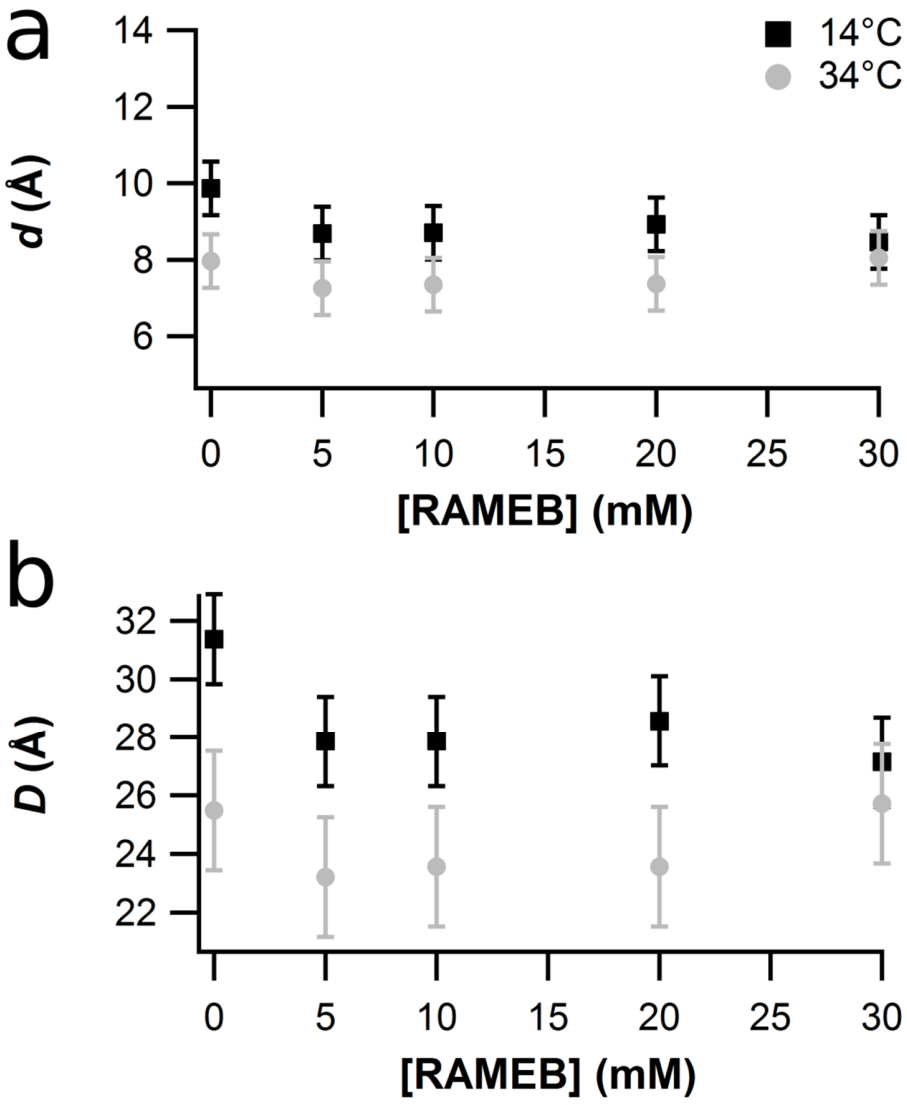

Fig. 7 DMPC sublayer thickness as a function of RAMEB concentration at 14°C (black squares) and 34°C (grey dots). (a) Average hydrophilic sublayer thickness; (b) Hydrophobic sublayer thickness

As inferred from the SANS data, the global thickness of the DMPC membranes in the absence of RAMEB is 41 ± 4Å at 34°C, with hydrophobic and hydrophilic contributions equal to respectively 25 ± 2 Å and 8,0 ± 0,9 Å. The membrane bilayer thickness of the same liposomes

increases at 14°C and reaches 51 ± 3 Å with hydrophobic and hydrophilic contributions which are respectively 31,4 ± 1,5 Å and 9,9 ± 0,7 Å. These results are in agreement with Kiselev's [64,72-74] and Kučerka's works [33]. It has to be kept in mind that the Luzzati thickness displayed in the latter reference cannot be directly compared to our value [75,76]. The larger value of the DMPC membrane thickness at 14°C is associated with the DMPC phase transition. At 14°C, the DMPC molecules are in a rigid and structured phase: the hydrophobic chains adopt elongated *anti*-conformations which optimize their mutual non-covalent interactions. The maximum chain-length for the DMPC hydrophobic moiety in an all *anti*-configuration is equal to 6×2,5Å=15Å, so that the hydrophobic sublayer is then expected to be 30Å thick which corresponds exactly to the observed hydrophobic thickness at 14°C. At 34°C, the phospholipid chains are in a fluid state leading to a thinner membrane because the entropic driving force favors *gauche* conformations leading to a more compact molecular shape. These results have been confirmed by several study [75,76].

DMPC extraction by RAMEB leads at 14°C to a decrease of the bilayer thickness of the surviving liposomes. On an absolute scale, the decrease is slightly more significant for the hydrophobic part than for the hydrophilic part. This decrease of the global bilayer thickness upon addition of RAMEB is compatible with the findings of our previous work [37]. At 34°C, no significant change could be inferred.

We suggest the following tentative mechanism, which is compatible with the results on the average radius presented in a Subsection 3.2. After phospholipid extraction by RAMEB, some liposomes are completely disrupted, some are not. Fig. 3 shows that, depending on the temperature, 25 to 45% of the liposomes are disrupted. They are either no longer detected in our SANS experiments or detected as RAMEB-DMPC inclusion complexes. In the surviving liposomes, the space made available by the extracted chains allows relaxation processes for the remaining ones. Intercalation of DMPC hydrophobic chains from the inner part of the liposome into the available free space of the outer part becomes possible. This space may also be used by their neighbor molecules which can now adopt a larger number of *gauche*-conformations and, as a consequence, a more compact shape leading to a thinner sublayer. From this point of view, it is logical that the long hydrophobic chains are more affected than the smaller polar heads, so that

the hydrophobic sublayer thickness decreases more upon RAMEB addition than the hydrophilic ones. At 34°C, above the bilayer transition temperature, it can be argued that the larger proportion of *gauche*-conformations already present without RAMEB, as mentioned above, makes the bilayer less prone to an additional thickness reduction.

4 Conclusions

The small angle neutron scattering technique has been applied to characterize the influence of a methylated β-cyclodextrin (RAMEB) on the structural parameters of DMPC liposomes. The SANS data are corroborated by DLS experiments but provide us with a more detailed picture of the liposome – cyclodextrin interactions.

The evolution of the fraction of DMPC molecules inserted in the liposomes, and of the aggregation number, confirms that RAMEB at a concentration larger than 10 mM is able to significantly affect the vesicles by extracting phospholipids in a dose dependent way. Information about the coverage of the liposome outer interface by RAMEB was also accessed: at 30 mM of RAMEB, about half of the liposome is covered. Part of the extracted DMPC chains becomes inserted into RAMEB-DMPC inclusion complexes. Part of them participates in the reorganization of the vesicles, leading to larger, more stable liposomes. The fact that the RAMEB influence becomes significant only for [RAMEB] > 10 mM is compatible with the conclusions of Anderson et al [60], who conclude to minimal phospholipid membrane disruption below 15 mM.

The important influence of the temperature on the phospholipidic extraction has been highlighted. Below the bilayer transition temperature, the average liposome radius increases upon addition of RAMEB, an observation which we interpret as a preferential disruption of the small vesicles by the CD and which we correlate with the different contributions to the bilayer bending energy in the framework of the Area-Difference-Elasticity model [67]. The polydispersity increase is assigned to the reorganization process involving random insertion of extracted DMPC chains into larger liposomes. Above the transition temperature, due to a much smaller bilayer bending modulus, all vesicles are suggested to be affected to the same extent by the interaction with RAMEB, which leaves the size distribution nearly unaffected.

The modelled SANS data allowed us to evaluate the effect of the CD on the DMPC membrane thickness below and above the transition temperature. At 14°C, addition of RAMEB leads to a decrease of the bilayer thickness, which is interpreted as a relaxation of the remaining chains in the space made available by the loss of the extracted ones. No significant effect is observed at 34°C.

Acknowledgments

This work is partly based on the experiments performed at the Jülich Centre for Neutron Science (JCNS) in Germany. The authors are grateful to JCNS for providing access to the its small angle neutron scattering instrumentation through the NMI3 network funded by the European Commission.We are grateful to Dr. M. Heinrich, Dr. M. A. Bahri and Prof. J.-P. Gaspard for their help in the neutron scattering experiments. The authors are grateful to the Centre for Study and Research on Macromolecules (CERM) and to the Structural Inorganic Chemistry Laboratory (LCIS) of the University of Liege (Belgium) for having made their DLS equipment available. We are also grateful to Marjorie Lismont (Laboratory of Biophotonics, University of Liège) for her help in the surface tension measurements. Constructive suggestions by the referees, in particular concerning inclusion complexes, are gratefully acknowledged.

References

1. Ohvo-Rekilä, H., Slotte, J.P.: Cyclodextrin-Mediated Removal of Sterols from Monolayers: Effects of Sterol Structure and Phospholipids on Desorption Rate. Biochem **35**, 8018-8024 (1996).
2. Villiers, A.: Sur la transformation de la fécule en dextrine par le ferment butyrique. Compt. Rend. Fr. Acad. Sci. **112**, 536-538 (1891).
3. Cramer, F.: Einschlussverbindungen. Berlin (1954)
4. Schardinger, F.: kristallisierter Polysaccharide (Dextrine) aus Starkekleister durch Microben. Zentralbl. Bakteriol. Parasitenk. Abt. **29**, 188-197 (1911).
5. Gabelica, V., Galic, N., De Pauw, E.: On the specificity of cyclodextrin complexes detected by electrospray mass spectrometry. J. Am. Soc. Mass. Spectrom. **13**, 946-953 (2002).
6. Loftsson, T., Brewster, M.E.: Pharmaceutical applications of cyclodextrins. 1. Drug solubilization and stabilization. Journal of Pharmaceutical Sciences **85**(10), 1017-1025 (1996). doi:10.1021/js950534b
7. Hashimoto, H.: Present Status of Industrial Application of Cyclodextrins in Japan. J. Inclusion Phenom. Macrocyclic Chem. **44**, 57-62 (2002).
8. Buschmann, H.-J., Schollmeyer, E.: Applications of cyclodextrins in cosmetic products: A review. J. Cosmet. Sci. **53**, 185-191 (2002).
9. Hedges, A.R.: Industrial Applications of Cyclodextrins. Chem. Rev. **98**, 2035-2044 (1998).
10. Szejtli, J.: past, present and future of cyclodextrin research. Pure and Applied Chemistry **76**, 1825-1845 (2004).
11. Szejtli, J.: Cyclodextrins in the Textile Industry. Starch **55**, 191-196 (2003).
12. Loftsson, T., Brewster, M.E.: Pharmaceutical applications of cyclodextrins: basic science and product development. J Pharm Pharmacol **62**(11), 1607-1621 (2010). doi:10.1111/j.2042-7158.2010.01030.x
13. Loftsson, T., Duchene, D.: Cyclodextrins and their pharmaceutical applications. Int J Pharm **329**(1-2), 1-11 (2007). doi:10.1016/j.ijpharm.2006.10.044
14. Zarrabi, A., Vossoughi, M.: Paclitaxel/β-CD-g-PG inclusion complex: An insight into complexation thermodynamics and guest solubility. Journal of Molecular Liquids **208**, 145-150 (2015). doi:10.1016/j.molliq.2015.04.019
15. Brewster, M.E., Loftsson, T.: Cyclodextrins as pharmaceutical solubilizers. Adv Drug Deliv Rev **59**(7), 645-666 (2007). doi:DOI: 10.1016/j.addr.2007.05.012
16. Castagne, D., Fillet, M., Delattre, L., Evrard, B., Nusgens, B., Piel, G.: Study of the cholesterol extraction capacity of β-cyclodextrin and its derivatives, relationships with their effects on endothelial cell viability and on membrane models J Incl Phenom Macrocycl Chem **63**(225-231) (2008).
17. Graham, D.R.M., Chertova, E., Hilburn, J.M., Arthur, L.O., Hildreth, J.E.K.: Cholesterol Depletion of Human Immunodeficiency Virus Type 1 and Simian Immunodeficiency Virus with β-Cyclodextrin Inactivates and Permeabilizes the Virions: Evidence for Virion-Associated Lipid Rafts. J. Virology **77**, 8237-8248 (2003).
18. Zidovetzki, R., Levitan, I.: Use of cyclodextrins to manipulate plasma membrane cholesterol content: evidence, misconceptions and control strategies. Biochim Biophys Acta **1768**(6), 1311-1324 (2007). doi:10.1016/j.bbamem.2007.03.026

19. Hatzi, P., Mourtas, S., Klepetsanis, P.G., Antimisiaris, S.G.: Study of the interaction between cyclodextrins and liposome membranes: effect on the permeability of liposomes. International Journal of Pharmaceutics **225**, 15-30 (2007).
20. Loftsson, T., Masson, M.: Cyclodextrins in topical drug formulation: theory and pratice. International Journal of Pharmaceutics **225**, 15-30 (2001).
21. Grammenos, A., Mouithys-Mickalad, A., Guelluy, P.H., Lismont, M., Piel, G., Hoebeke, M.: ESR technique for noninvasive way to quantify cyclodextrins effect on cell membranes. Biochem Biophys Res Commun **398**(3), 350-354 (2010). doi:10.1016/j.bbrc.2010.06.050
22. Piel, G., Moutard, S., Uhoda, E., Pilard, F., Pierard, G.E., Perly, B., Delattre, L., Evrard, B.: Skin compatibility of cyclodextrins and their derivatives: a comparative assessment using a corneoxenometry bioassay. Eur J Pharm Biopharm **57**(3), 479-482 (2004). doi:10.1016/j.ejpb.2003.12.004
23. Piel, G., Piette, M., Barillaro, V., Castagne, D., Evrard, B., Delattre, L.: Study of the relationship between lipid binding properties of cyclodextrins and their effect on the integrity of liposomes. Int J Pharm **338**(1-2), 35-42 (2007). doi:10.1016/j.ijpharm.2007.01.015
24. Lê-Quôc, D.a.L.-Q.K.: http://www.espacesciences.com/index.html. (2000).
25. He, Y., Fu, P., Shen, X., Gao, H.: Cyclodextrin-based aggregates and characterization by microscopy. Micron **39**, 495-516 (2008).
26. Messner, M., Kurkov, S.V., Jansook, P., Loftsson, T.: Self-assembled cyclodextrin aggregates and nanoparticles. International Journal of Pharmaceutics **387**, 199-208. (2010).
27. Kučerka, N., Pencer, J., Sachs, J., Nagle, J., Katsaras, J.: Curvature effect on the structure of phospholipid bilayer. Langmuir **23**, 1292-1299. (2007).
28. Kučerka, N., Nieh, M., Pencer, J., Harroun, T., Katsaras, J.: The study of liposomes, Lamellae and Membranes Using Neutrons and X-rays. Curr Opin Colloid Int **12**, 17-22 (2007).
29. Pabst, G., Kučerka, N., Nieh, M., Rheinstädter, M., Katsaras, J.: Application of neutrons and X-ray scattering to the study of biologically relevant model membranes. Chem. Phys. Lipids **163**, 460-479 (2010).
30. Kučerka, N., Kiselev, M.a., Balgavý, P.: Determination of bilayer thickness and lipid surface area in unilamellar dimyristoylphosphatidylcholine vesicles from small-angle neutron scattering curves: a comparison of evaluation methods. European biophysics journal : EBJ **33**, 328-334 (2004). doi:10.1007/s00249-003-0349-0
31. Kučerka, N., Liu, Y., Chu, N., Petrache, H.I., Tristram-Nagle, S., Nagle, J.F.: Structure of fully hydrated fluid phase DMPC and DLPC lipid bilayers using X-ray scattering from oriented multilamellar arrays and from unilamellar vesicles. Biophysical journal **88**, 2626-2637 (2005). doi:10.1529/biophysj.104.056606
32. Kučerka, N., Nagle, J.F., Sachs, J.N., Feller, S.E., Pencer, J., Jackson, A., Katsaras, J.: Lipid bilayer structure determined by the simultaneous analysis of neutron and X-ray scattering data. Biophysical journal **95**, 2356-2367 (2008). doi:10.1529/biophysj.108.132662
33. Kučerka, N., Nieh, M.P., Katsaras, J.: Fluid phase lipid areas and bilayer thicknesses of commonly used phosphatidylcholines as a function of temperature. Biochimica et Biophysica Acta - Biomembranes **1808**, 2761-2771 (2011). doi:10.1016/j.bbamem.2011.07.022

34. Belička, M., Devínsky, F., Balgavý, P.: Neutrons in studies of phospholipid bilayers and bilayer–drug interaction. II. Small-angle scattering. Acta Facultatis Pharmaceuticae Universitatis Comenianae **61**, 12-20 (2014). doi:10.2478/afpuc-2014-0011
35. Belička, M., Devínsky, F., Balgavý, P.: Neutrons in studies of phospholipid bilayers and bilayer–drug interaction. I. Basic principles and neutron diffraction. Acta Facultatis Pharmaceuticae Universitatis Comenianae **61**, 1-11 (2014). doi:10.2478/afpuc-2014-0010
36. Uhríková, D., Kučerka, N., Teixeira, J., Gordeliy, V., Balgavý, P.: Structural changes in dipalmitoylphosphatidylcholine bilayer promoted by Ca2+ ions: a small-angle neutron scattering study. Chemistry and Physics of Lipids **155**, 80-89 (2008). doi:10.1016/j.chemphyslip.2008.07.010
37. Grammenos, A., Bahri, M.A., Guelluy, P.H., Piel, G., Hoebeke, M.: Quantification of Randomly-methylated-beta-cyclodextrin effect on liposome: an ESR study. Biochem Biophys Res Commun **390**(1), 5-9 (2009). doi:10.1016/j.bbrc.2009.08.172
38. Guelluy, P.H., Fontaine-Aupart, M.P., Grammenos, A., Lecart, S., Piette, J., Hoebeke, M.: Optimizing photodynamic therapy by liposomal formulation of the photosensitizer pyropheophorbide-a methyl ester: in vitro and ex vivo comparative biophysical investigations in a colon carcinoma cell line. Photochem Photobiol Sci **9**(9), 1252-1260 (2010). doi:10.1039/c0pp00100g
39. Vrhovnik, K., Kristl, J., Sentjurc, M., Smid-Korbar, J.: Influence of liposome bilayer fluidity on the transport of encapsulated substance into the skin as evaluated by EPR. Pharm Res **15**(4), 525-530 (1998).
40. Battistini, L., Burreddu, P., Sartori, A., Arosio, D., Manzoni, L., Paduano, L., Derrico, G., Sala, R., Reia, L., Bonomini, S., Rassu, G., Zanardi, F.: Enhancement of the uptake and cytotoxic activity of doxorubicin in cancer cells by novel cRGD-semipeptide-anchoring liposomes. Molecular Pharmaceutics **11**, 2280-2293 (2014). doi:10.1021/mp400718j
41. Etheridge, M.L., Campbell, S.a., Erdman, A.G., Haynes, C.L., Wolf, S.M., McCullough, J.: The big picture on nanomedicine: the state of investigational and approved nanomedicine products. Nanomedicine : nanotechnology, biology, and medicine **9**, 1-14 (2013). doi:10.1016/j.nano.2012.05.013
42. Ntimenou, V., Fahr, A., Antimisiaris, S.G.: Elastic vesicles for transdermal drug delivery of hydrophilic drugs: a comparison of important physicochemical characteristics of different vesicle types. Journal of biomedical nanotechnology **8**(4), 613-623 (2012).
43. Mourtas, S., Mao, J., Parsy, C.C., Storer, R., Klepetsanis, P., Antimisiaris, S.G.: Liposomal gels for vaginal delivery of the microbicide MC-1220: preparation and in vivo vaginal toxicity and pharmacokinetics. Nano Life **1**(03n04), 195-205 (2010).
44. Boulmedarat, L., Piel, G., Bochot, A., Lesieur, S., Delattre, L., Fattal, E.: Cyclodextrin-mediated drug release from liposomes dispersed within a bioadhesive gel. Pharm Res **22**(6), 962-971 (2005). doi:10.1007/s11095-005-4591-2
45. Gillet, A., Grammenos, A., Compere, P., Evrard, B., Piel, G.: Development of a new topical system: drug-in-cyclodextrin-in-deformable liposome. Int J Pharm **380**(1-2), 174-180 (2009). doi:10.1016/j.ijpharm.2009.06.027
46. Gharib, R., Greige-Gerges, H., Fourmentin, S., Charcosset, C., Auezova, L.: Liposomes incorporating cyclodextrin-drug inclusion complexes: current state of knowledge. Carbohydrate Polymers **129**, 175-186 (2015). doi:10.1016/j.carbpol.2015.04.048

47. Piel, G., Piette, M., Barillaro, V., Castagne, D., Evrard, B., Delattre, L.: Betamethasone-in-cyclodextrin-in-liposome: the effect of cyclodextrins on encapsulation efficiency and release kinetics. Int J Pharm **312**(1-2), 75-82 (2006). doi:10.1016/j.ijpharm.2005.12.044
48. Tsamaloukas, A., Szadkowska, H., Slotte, J.P., Heerklotz, H.: Interaction of cholesterol with lipid membranes and cyclodextrin charaterized by calorimetry. Biophys J **89**, 1109-1119 (2005).
49. Puskás, I., Barcza, L., Szente, L., Csempesz, F.: Features of the Interaction between Cyclodextrins and Colloidal Liposomes. Journal of Inclusion Phenomena and Macrocyclic Chemistry **54**(1-2), 89-93 (2006). doi:10.1007/s10847-005-4805-6
50. Piette, M., Evrard, B., Frankenne, F., Chiap, P., Bertholet, P., Castagne, D., Foidart, J.M., Delattre, L., Piel, G.: Pharmacokinetic study of a new synthetic MMP inhibitor (Ro 28-2653) after IV and oral administration of cyclodextrin solutions. Eur J Pharm Sci **28**(3), 189-195 (2006). doi:10.1016/j.ejps.2006.01.011
51. Hatzi, P., Mourtas, S., G. Klepetsanis, P., Antimisiaris, S.G.: Integrity of liposomes in presence of cyclodextrins: Effect of liposome type and lipid composition. International Journal of Pharmaceutics **333**, 167-176 (2007). doi:10.1016/j.ijpharm.2006.09.059
52. Caffrey, M., Hogan, J.: LIPIDAT: A database of lipid phase transition temperatures and enthalpy changes. DMPC data subset analysis. Lipids **61**, 1-109 (1992).
53. Hope, M., Bally, M., Webb, G., Cullis, P.: Production of large unilamellar vesicles by rapid extrusion procedure. Characterization of size distribution, trapped volume and ability to maintain a membrane potential. Biochem Biophys Acta **812**, 55-65 (1985).
54. Lentz, B., Carpenter, T., Alford, D.: Spontaneous fusion of phosphatidylcholine small unilamellar vesicles in the fluid phase. Biochem **26**, 5389-5397 (1987).
55. Coderch, L., Fonollosa, J., De Pera, M., Estelrich, J., De La Maza, A., Parra, J.L.: Influence of cholesterol on liposome fluidity by EPR. Relationship with percutaneous absorption. J Control Release **68**(1), 85-95 (2000). doi:10.1016/S0168-3659(00)00240-6
56. Olson, F., Hunt, C.A., Szoka, F.C., Vail, W.J., Papahadjopoulos, D.: Preparation of liposomes of defined size distribution by extrusion through polycarbonate membranes. Biochim Biophys Acta **557**(1), 9-23 (1979).
57. Brûlet, A., Lairez, D., Lapp, A., Cotton, J.-P.: Improvement of data treatment in small-angle neutron scattering. J Appl crystallogr **40**, 165-177 (2007).
58. Hammouda, B.: Probing nanoscale structures - The SANS tollbox. National Institute of Standards and Technology Center for Neutron Research Gaithersburg (2009)
59. Szejtli, J.: Introduction and General Overview of Cyclodextrin Chemistry. Chem. Rev. **98**, 1743-1753 (1998). doi:10.1021/CR970022C
60. Anderson, T.G., Tan, A., Ganz, P., Seelig, J.: Calorimetric Measurement of Phospholipid Interaction with Methyl-beta-Cyclodextrin. Biochemistry **43**, 2251-2261 (2004). doi:10.1021/bi0358869
61. Hallett, A.F., Craig, T., Marsh, J., Nickel, B.: Number Distributions by Dynamic Light Scattering. Can. J. Spectr. **34**, 63-70 (1989).
62. Maulucci, G., De Spirito, M., Arcovito, G., Boffi, F., Castellano, A.C., Briganti, G.: Particle size distribution in DMPC vesicles solutions undergoing different sonication times. Biophys. J. **88**, 3545-3550 (2005).

63. González-Gaitano, G., da Silva, M.a., Radulescu, A., Dreiss, C.a.: Selective Tuning of the Self-Assembly and Gelation of a Hydrophilic Poloxamine by Cyclodextrins. Langmuir **31**, 5645-5655 (2015). doi:10.1021/acs.langmuir.5b01081
64. Kiselev, M.A., Zemlyanaya, E.V., Aswal, V.K., Neubert, R.H.: What can we learn about the lipid vesicle structure from the small-angle neutron scattering experiment? Eur Biophys J **35**, 477-493 (2006).
65. Másson, M., Loftsson, T., Másson, G., Stefánsson, E.: Cyclodextrins as permeation enhancers: some theoretical evaluations and in vitro testing. Journal of Controlled Release **59**(1), 107-118 (1999). doi:Doi: 10.1016/s0168-3659(98)00182-5
66. Puskas, I., Csempesz, F.: Influence of cyclodextrins on the physical stability of DPPC-liposomes. Colloids and Surfaces B: Biointerfaces **58**(2), 218-224 (2007). doi:10.1016/j.colsurfb.2007.03.011
67. Miao, L., Seifert, U., Wortis, M., Döbereiner, H.-G.: Budding transitions of fluid-bilayer vesicles:The effect of area-difference elasticity. Phys. Rev. E **49**, 5389-5407 (1996).
68. Helfrich, W. Z. Naturforsch. C **28**, 693 (1973).
69. Morse, D.C., Milner, S.T.: Statistical mechanics of closed fluid membranes. Phys. Rev. E **52**, 5918-5945 (1995).
70. Charitat, T., Lecuyer, S., Fragneto, G.: Fluctuation and destabilization of single phospholipids bilayers. Biointerphases **3**, FB3-FB15 (2008).
71. Mascetti, J., Castano, S., Cavagnat, D., Desbat, B.: Organization of β-Cyclodextrin under Pure Cholesterol, DMPC, or DMPG and Mixed Cholesterol/Phospholipid Monolayers. Langmuir **24**(17), 9616-9622 (2008). doi:10.1021/la8004294
72. Kiselev, M.A., Zemlyanaya, E.V., Aswal, V.K.: Sans study of the unilamellar DMPC vesicles. The fluctuation model of lipid bilayer. Crystallography reports (2004).
73. Kiselev, M.A., Zbytovska, J., Matveev, D., Wartewig, S., Gapienko, I.V., Perez, J., Lesieur, P., Hoell, A., Neubert, R.: Influence of trehalose on the structure of unilamellar DMPC vesicles. Colloids and Surfaces A: Physicochemical and Engineering Aspects **256**(1), 1-7 (2005). doi:DOI: 10.1016/j.colsurfa.2004.09.017
74. Kucerka, N., Kiselev, M.A., Balgavy, P.: Determination of bilayer thickness and lipid surface area in unilamellar dimyristoylphosphatidylcholine vesicles from small-angle neutron scattering curves: a comparison of evaluation methods. Eur Biophys J **33**(4), 328-334 (2004). doi:10.1007/s00249-003-0349-0
75. Nagle, J.F., Tristram-Nagle, S.: Lipid Bilayer Structure. Current opinion in structural biology **10**, 474-480 (2000).
76. Nagle, J., Petrache, H., Gouliaev, N., Tristram-Nagle, S., Liu, Y., Suter, R., Gawrisch, K.: Multiple mechanisms for critical behavior in the biologically relevant phase of lecithin bilayers. Physical Review E **58**, 7769-7776 (1998). doi:10.1103/PhysRevE.58.7769